J. Plasma Phys. (2016), *vol.* 82, 905820108
doi:10.1017/S0022377816000076

Nonlinear electrostatic solitary waves in electron–positron plasmas

I. J. Lazarus[1,†], R. Bharuthram[2], S. Moolla[3], S. V. Singh[4] and G. S. Lakhina[4]

[1]Department of Physics, Durban University of Technology, Durban 4001, South Africa

[2]University of the Western Cape, Modderdam Road, Bellville 7530, South Africa

[3]School of Physics, University of KwaZulu-Natal, Durban 4000, South Africa

[4]Indian Institute of Geomagnetism, Navi Mumbai 401206, India

(Received 5 December 2014; revised 14 January 2016; accepted 14 January 2016)

The generation of nonlinear electrostatic solitary waves (ESWs) is explored in a magnetized four component two-temperature electron–positron plasma. Fluid theory is used to derive a set of nonlinear equations for the ESWs, which propagate obliquely to an external magnetic field. The electric field structures are examined for various plasma parameters and are shown to yield sinusoidal, sawtooth and bipolar waveforms. It is found that an increase in the densities of the electrons and positrons strengthen the nonlinearity while the periodicity and nonlinearity of the wave increases as the cool-to-hot temperature ratio increases. Our results could be useful in understanding nonlinear propagation of waves in astrophysical environments and related laboratory experiments.

1. Introduction

In the last few decades, electron–positron (e–p) plasmas have attracted significant interest amongst researchers. The study of nonlinear effects in e–p plasmas is important since it is known that these plasmas exists in pulsars (Goldreich & Julian 1969; Michel 1982), active galactic nuclei (Miller & Witta 1987), gamma-ray bursts (GRBs) (Piran 2005), white dwarfs (Kashiyama, Ioka & Kawanaka 2011) and have also been studied in laboratory experiments (Greaves & Surko 1995). In these plasmas, there exists only one frequency scale, due to the same charge-to-mass ratio for the oppositely charged species. Hence they are different from their electron–ion counterparts and thus exhibit different wave phenomena.

It is thought that most of the e–p plasmas produced in astrophysical settings are of relativistic nature. The process by which a pulsar magnetosphere is populated with relativistic e–p plasma is assumed to be the decay of photons emitted by primary particles into secondary pairs. Synchrotron emission from these secondary pairs is then assumed to contribute to the high-energy emission from some pulsars. The choice of a relativistic or non-relativistic character for the distribution function of the involved particles is intimately related to the process of formation of the pairs

† Email address for correspondence: lazarusi@dut.ac.za

(Asseo & Riazuelo 2000; Weise & Melrose 2002). It is, therefore, plausible that non-relativistic astrophysical e–p plasmas may exist, given the effect of efficient cooling by cyclotron emissions (Zank & Greaves 1995; Bhattacharyya, Janaki & Dasgupta 2003). There is a vast body of literature dealing with linear and nonlinear wave propagation in e–p plasmas which are non-relativistic (Iwamoto 1993; Zank & Greaves 1995; Verheest *et al.* 1996; Esfandyari-Kalejahi, Kourakis & Shukla 2006). A simple two-fluid model was used to study the linear and nonlinear wave phenomena in electrostatic and electromagnetic solitary waves by Zank & Greaves (1995). This linear study showed that many wave phenomena found in conventional electron–ion plasmas exist in a modified form in e–p plasmas. In their nonlinear analysis they found that only subsonic solutions exist, while the pulse width, rather than its amplitude, is related to the wave speed. Their results also showed that increasing the Mach number narrows the pulse width significantly, without any change in the amplitude.

Lu *et al.* (2010) investigated nonlinear electrostatic waves in an e–p plasma in the presence of background ions. They found that both smooth and spiky quasistationary waves were found to exist. They reported that as the wave speed increases, the nonlinearity of the wave decreases. They also pointed out that their results may be useful in understanding astrophysical and laboratory wave phenomena involving pair production and positron emissions. Liu & Liu (2011) investigated the formation of large-amplitude electromagnetic solitons with spiky structures in e–p plasmas. They pointed out that the localized electric field structures are important in understanding astrophysical objects, which could account for pulsar radio emissions. Spiky Langmuir solitons in a dense ultrarelativistic e–p plasma have been studied by Mofiz & Mamun (1992) and Mofiz & Amin (2013). Mofiz & Amin (2013) used the two-fluid magnetohydrodynamic (MHD) equations to describe the e–p plasma, and found spiky Langmuir solitons that propagated along the open field lines of a pulsar magnetosphere, indicating that there is some association with pulsar radio emissions. Stark *et al.* (2007) investigated a possible emission mechanism through the coupling of electrostatic oscillations with propagating electromagnetic waves using an e–p plasma model relevant to pulsar magnetospheres.

On the other hand, satellite observations in the Earth's magnetosphere have also shown the existence of electrostatic solitary waves as part of broadband electrostatic noise (BEN). The (GEOTAIL (Matsumoto *et al.* 1994, 1997; Kojima *et al.* 1999), POLAR (Franz, Kintner & Pickett 1998) and FAST (Ergun *et al.* 1998)) satellites frequently observed BEN and ESWs in various regions of the Earth's magnetosphere. The characteristic feature of ESWs is solitary bipolar pulses and consist of small scale, large amplitude, parallel electric fields. These large-amplitude spiky structures have been interpreted in terms of either solitons (Temerin *et al.* 1982) or isolated electron holes in the phase space corresponding to positive electrostatic potential (Omura *et al.* 1994). Given that e–p plasmas are increasingly observed in astrophysical environments, as well as in laboratory experiments, the above mentioned satellite observations also lead us to explore if such nonlinear structures are also possible in e–p plasmas.

There is a distinct possibility that a pulsar magnetosphere can support the coexistence of two types of cold and hot e–p populations (Sturrock 1971; Bharuthram 1992; Lazarus *et al.* 2012). Linear electrostatic waves (Lazarus *et al.* 2012) and solitary waves (Lazarus, Bharuthram & Hellberg 2008) have been studied in such a system. Here, we will investigate the possibility of nonlinear electrostatic spiky structures in a magnetized four component two-temperature e–p plasma. The paper is structured as follows. In § 2, the basic equations for the e–p plasma are presented. In § 3 we present the numerical results. A summary of our findings is presented in § 4.

2. Basic theory

The model considered here is a homogeneous magnetized, four component, collisionless, e–p plasma, consisting of cool electrons (ec) and cool positrons (pc) with equal temperatures T_c and initial densities ($n_{ec0} = n_{pc0}$), and hot electrons (eh) and hot positrons (ph) with equal temperatures T_h and densities ($n_{eh0} = n_{ph0}$). Wave propagation is taken in the x-direction at an angle θ to the magnetic field $\boldsymbol{B}_0$, which is assumed to be in the x–z plane.

The continuity and momentum equations for the four species are given by

$$\frac{\partial n_j}{\partial t} + \frac{\partial (n_j v_{jx})}{\partial x} = 0 \tag{2.1}$$

$$\frac{\partial v_{jx}}{\partial t} + v_{jx}\frac{\partial v_{jx}}{\partial x} + \frac{1}{n_j m}\frac{\partial p_j}{\partial x} = -\frac{\epsilon_j e}{m}\frac{\partial \phi}{\partial x} + \epsilon_j \Omega v_{jy} \sin\theta \tag{2.2}$$

$$\frac{\partial v_{jy}}{\partial t} + v_{jx}\frac{\partial v_{jy}}{\partial x} = \epsilon_j \Omega v_{jz}\cos\theta - \epsilon_j \Omega v_{jx}\sin\theta \tag{2.3}$$

$$\frac{\partial v_{jz}}{\partial t} + v_{jx}\frac{\partial v_{jz}}{\partial x} = -\epsilon_j \Omega v_{jy}\cos\theta, \tag{2.4}$$

where $\epsilon_j = +1(-1)$ for positrons (electrons) and $j = ec, pc, eh, ph$ for the cool electrons, cool positrons, hot electrons and the hot positrons, respectively.

The density of the cool electrons (positrons) is n_{ec} (n_{pc}), and that of the hot electrons (positrons) is n_{eh} (n_{ph}).

The general equation of state for the four species is given by

$$\frac{\partial p_j}{\partial t} + v_{jx}\frac{\partial p_j}{\partial x} + 3p_j\frac{\partial v_{jx}}{\partial x} = 0. \tag{2.5}$$

The system is closed by the Poisson equation

$$\varepsilon_0 \frac{\partial^2 \phi}{\partial x^2} = -e(n_{pc} - n_{ec} + n_{ph} - n_{eh}). \tag{2.6}$$

In the above equations, n_j, $\boldsymbol{v}_j$ and p_j are the densities, fluid velocities and pressures, respectively, of the jth species. $\Omega = \Omega_e = \Omega_p = eB_0/m$ is the cyclotron frequency. Here $m = m_e = m_p$ is the common mass of the electrons and the positrons. Adiabatic compression, $\gamma = (2+N)/N = 3$, is assumed, where $N = 1$ implies one degree of freedom.

2.1. *Linear analysis*

Linearizing and combining equations (2.1)–(2.6) yields the following general dispersion relation for a four component e–p plasma:

$$\omega^2 = \frac{2\omega_{pc}^2(\omega^2 - \Omega^2\cos^2\theta)}{\omega^2 - \Omega^2 - \dfrac{3k^2 v_{tc}^2}{\omega^2}(\omega^2 - \Omega^2\cos^2\theta)} + \frac{2\omega_{ph}^2(\omega^2 - \Omega^2\cos^2\theta)}{\omega^2 - \Omega^2 - \dfrac{3k^2 v_{th}^2}{\omega^2}(\omega^2 - \Omega^2\cos^2\theta)}, \tag{2.7}$$

where $\omega_{pc,ph} = (n_{0c,h}e^2/\varepsilon_0 m)^{1/2}$ are the plasma frequencies of the cool and hot species, respectively.

In the limit $v_{tc} \ll \omega/k \ll v_{th}$, where $v_{th} = (T_h/m)^{1/2}$ and $v_{tc} = (T_c/m)^{1/2}$ are the thermal velocities of the hot (cool) species, the dispersion relation (2.7) becomes,

$$\omega^4 - \omega^2(\Omega^2 + 2\omega_s^2 + 3k^2v_{tc}^2) + 2\omega_s^2\Omega^2\cos^2\theta = 0, \tag{2.8}$$

where $\omega_s = \omega_{pc}/(1 + 2/3k^2\lambda_{Dh}^2)^{1/2}$ and $\lambda_{Dh} = (\varepsilon_0 T_h/n_{oh}e^2)^{1/2}$.

Equation (2.8) yields

$$\omega^2 = \frac{1}{2}(\Omega^2 + 2\omega_s^2 + 3k^2v_{tc}^2)\left[1 \pm \sqrt{1 - \frac{(8\omega_s^2\Omega^2\cos^2\theta)}{(\Omega^2 + 2\omega_s^2 + 3k^2v_{tc}^2)^2}}\right]. \tag{2.9}$$

In the limit $(8\omega_s^2\Omega^2\cos^2\theta) \ll (\Omega^2 + 2\omega_s^2 + 3k^2v_{tc}^2)^2$, (2.9) yields two modes. The positive sign gives the cyclotron mode,

$$\omega_+^2 = (\Omega^2 + 2\omega_s^2 + 3k^2v_{tc}^2) - \frac{2\omega_s^2\Omega^2\cos^2\theta}{\Omega^2 + 2\omega_s^2 + 3k^2v_{tc}^2} \tag{2.10}$$

and the negative sign gives the acoustic mode,

$$\omega_-^2 = \frac{2\omega_s^2\Omega^2\cos^2\theta}{\Omega^2 + 2\omega_s^2 + 3k^2v_{tc}^2}. \tag{2.11}$$

2.2. *Nonlinear analysis*

In the nonlinear regime, a transformation to a stationary frame $s = (x - Vt)(\Omega/V)$ is performed, and v, t, x and ϕ are normalized with respect to v_{th}, Ω^{-1}, $\rho = v_{th}/\Omega$, and T_h/e, respectively. V is the phase velocity of the wave. In (2.1)–(2.5), $\partial/\partial t$ is replaced by $-\Omega(\partial/\partial s)$ and $\partial/\partial x$ by $(\Omega/V)(\partial/\partial s)$, and the diving electric field amplitude is defined as $E = -(\partial\psi/\partial s)$, where $\psi = e\phi/T_h$.

Integrating equation (2.1) and using the initial conditions $n_{ec0} = n_0$ and $v_{ecx} = v_0$ at $s = 0$, yields the normalized velocity for the cool electrons in the x-direction.

$$v_{ecx} = -\left(\frac{n_{eco}}{n_{ec}}\right)(V - v_0) + V. \tag{2.12}$$

Similarly the cool positron, hot electron and hot positron velocities are determined. Substituting these into the normalized form of (2.2)–(2.5) gives the following set of nonlinear first-order differential equations in the stationary frame.

$$\frac{\partial\psi}{\partial s} = -E \tag{2.13}$$

$$\frac{\partial E}{\partial s} = R^2M^2(n_{pcn} - n_{ecn} + n_{phn} - n_{ehn}) \tag{2.14}$$

$$\frac{\partial n_{ecn}}{\partial s} = \frac{n_{ecn}^3[E + M\sin\theta v_{ecyn}]}{\left(\frac{n_{ec0}}{n_0}\right)^2(M - \delta_c)^2 - 3\frac{T_c}{T_h}p_{ecn}n_{ecn}} \tag{2.15}$$

$$\frac{\partial v_{ecyn}}{\partial s} = \left(\frac{n_0}{n_{ec0}}\right)\frac{Mn_{ecn}}{(M - \delta_c)}\left[-\left(M - \frac{(M - \delta_c)}{n_{ecn}}\left(\frac{n_{ec0}}{n_0}\right)\right)\sin\theta + v_{eczn}\cos\theta\right] \tag{2.16}$$

$$\frac{\partial v_{eczn}}{\partial s} = -\left(\frac{n_0}{n_{ec0}}\right)\frac{n_{ecn}v_{ecyn}M\cos\theta}{(M-\delta_c)} \tag{2.17}$$

$$\frac{\partial p_{ecn}}{\partial s} = \frac{3p_{ecn}n_{ecn}^2[E+M\sin\theta v_{ecyn}]}{\left(\dfrac{n_{ec0}}{n_0}\right)^2(M-\delta_c)^2 - 3\dfrac{T_c}{T_h}p_{ecn}n_{ecn}} \tag{2.18}$$

$$\frac{\partial n_{pcn}}{\partial s} = \frac{n_{pcn}^3[-E-M\sin\theta v_{pcyn}]}{\left(\dfrac{n_{pc0}}{n_0}\right)^2(M-\delta_c)^2 - 3\dfrac{T_c}{T_h}p_{pcn}n_{pcn}} \tag{2.19}$$

$$\frac{\partial v_{pcyn}}{\partial s} = \left(\frac{n_0}{n_{pc0}}\right)\frac{Mn_{pcn}}{(M-\delta_c)}\left[\left(M-\frac{(M-\delta_c)}{n_{pcn}}\left(\frac{n_{pc0}}{n_0}\right)\right)\sin\theta - v_{pczn}\cos\theta\right] \tag{2.20}$$

$$\frac{\partial v_{pczn}}{\partial s} = \left(\frac{n_0}{n_{pc0}}\right)\frac{n_{pcn}v_{pcyn}M\cos\theta}{(M-\delta_c)} \tag{2.21}$$

$$\frac{\partial p_{pcn}}{\partial s} = \frac{3p_{pcn}n_{pcn}^2[-E-M\sin\theta v_{pcyn}]}{\left(\dfrac{n_{pc0}}{n_0}\right)^2(M-\delta_c)^2 - 3\dfrac{T_c}{T_h}p_{pcn}n_{pcn}} \tag{2.22}$$

$$\frac{\partial p_{phn}}{\partial s} = \frac{3p_{phn}n_{phn}^2[-E-M\sin\theta v_{phyn}]}{\left(\dfrac{n_{ph0}}{n_0}\right)^2(M-\delta_h)^2 - 3p_{phn}n_{phn}} \tag{2.23}$$

$$\frac{\partial n_{phn}}{\partial s} = \frac{n_{phn}^3[-E-M\sin\theta v_{phyn}]}{\left(\dfrac{n_{ph0}}{n_0}\right)^2(M-\delta_h)^2 - 3p_{phn}n_{phn}} \tag{2.24}$$

$$\frac{\partial v_{phyn}}{\partial s} = \left(\frac{n_0}{n_{ph0}}\right)\frac{Mn_{phn}}{(M-\delta_h)}\left[\left(M-\frac{(M-\delta_h)}{n_{phn}}\left(\frac{n_{ph0}}{n_0}\right)\right)\sin\theta - v_{phzn}\cos\theta\right] \tag{2.25}$$

$$\frac{\partial v_{phzn}}{\partial s} = \left(\frac{n_0}{n_{ph0}}\right)\frac{n_{phn}v_{phyn}M\cos\theta}{(M-\delta_h)} \tag{2.26}$$

$$\frac{\partial p_{ehn}}{\partial s} = \frac{3p_{ehn}n_{ehn}^2[E+M\sin\theta v_{ehyn}]}{\left(\dfrac{n_{eh0}}{n_0}\right)^2(M-\delta_h)^2 - 3p_{ehn}n_{ehn}} \tag{2.27}$$

$$\frac{\partial n_{ehn}}{\partial s} = \frac{n_{ehn}^3[E+M\sin\theta v_{ehyn}]}{\left(\dfrac{n_{eh0}}{n_0}\right)^2(M-\delta_h)^2 - 3p_{ehn}n_{ehn}} \tag{2.28}$$

$$\frac{\partial v_{ehn}}{\partial s} = \left(\frac{n_0}{n_{eh0}}\right)\frac{Mn_{ehn}}{(M-\delta_h)}\left[-\left(M-\frac{(M-\delta_h)}{n_{ehn}}\left(\frac{n_{eh0}}{n_0}\right)\right)\sin\theta + v_{ehzn}\cos\theta\right] \tag{2.29}$$

$$\frac{\partial v_{ehzn}}{\partial s} = -\left(\frac{n_0}{n_{eh0}}\right)\frac{n_{ehn}v_{ehyn}M\cos\theta}{(M-\delta_h)}. \tag{2.30}$$

In (2.13)–(2.30), the velocities are normalized with respect to the thermal velocity of the hot species $v_{th} = (T_h/m)^{1/2}$ and the densities with respect to the total density n_0. The equilibrium density of the cool (hot) electrons is n_{ec0} (n_{eh0}), and that of the cool (hot) positrons n_{pc0} (n_{ph0}), with $n_{ec0} + n_{eh0} = n_{pc0} + n_{ph0} = n_0$. $R = \omega_p/\Omega$, where

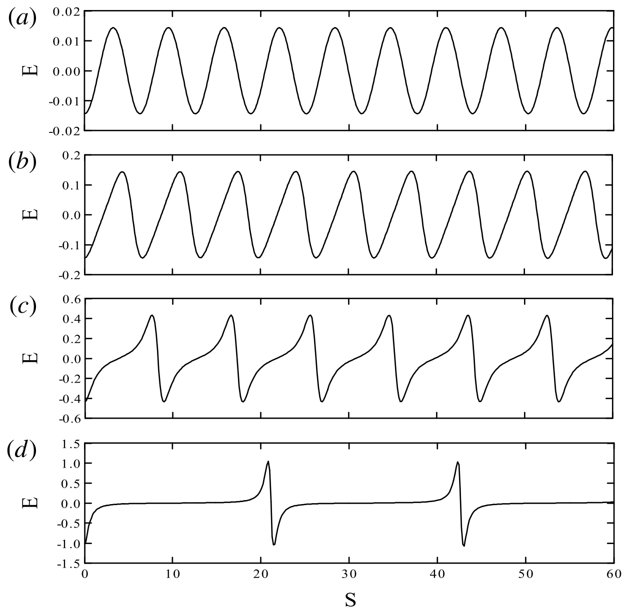

FIGURE 1. Numerical solution of the normalized electric field for the parameters $M = 3.5$, $\theta = 2°$, $R = 10.0$, $\delta_c = \delta_h = 0.0$, $n_{ec0}/n_0 = n_{pc0}/n_0 = 0.5$, $T_c/T_h = 0.0$, and $E_0 =$ (*a*) 0.05 (linear waveform), (*b*) 0.5 (sinusoidal waveform), (*c*) 1.5 (sawtooth waveform) and (*d*) 3.5 (bipolar waveform).

$\omega_p = (n_0 e^2/\varepsilon_0 m)^{1/2}$ is the total plasma frequency, $M = V/v_{th}$ is the Mach number and $\delta_{c,h} = v_{0c,0h}/v_{th}$ is the normalized drift velocity of cool (hot) species at $s = 0$.

3. Numerical results

The system of nonlinear first-order differential equations (2.13)–(2.30) are solved numerically using the Runge–Kutta (RK4) technique (Press *et al.* 1996). The initial values were determined self-consistently. All figures illustrate the actual normalized electric fields $E_{norm} = -(1/M)(\partial\psi/\partial s)$.

Figure 1(*a–d*) shows the evolution of the system for various driving electric field amplitudes E_0. The fixed parameters are $M = 3.5$, $R = 10.0$, $\theta = 2°$, $\delta_c = \delta_h = 0.0$, $n_{ec0}/n_0 = n_{pc0}/n_0 = 0.5$ and $T_c/T_h = 0.0$. Note that wave propagation is taken almost parallel to the ambient magnetic field $\boldsymbol{B}_0$. As E_0 increases, the electric field structure evolves from a sinusoidal wave to a sawtooth structure. For a higher E_0 value of 3.5, the potential structure has a spiky bipolar form. As E_0 increases, the period of the wave increases and the frequency decreases. The period of oscillations is given by $\Delta S = (\Delta x - V\Delta t)(\Omega/V)$. Typically for $\Delta x = 0$, $\Delta S = |\Omega\Delta t|$. Hence for the linear wave in figure 1(*a*), with a small driving amplitude of $E_0 = 0.05$, the period of the wave is calculated to be $T_w = 0.995\tau_c$ (frequency $f_w = 1.0 f_c$), displaying the cyclotron mode, where $\tau_c = 2\pi/\Omega$. In figure 1(*b*), for $E_0 = 0.5$, $T_w = 1.12\tau_c$ (frequency $f_w = 0.89 f_c$). Figure 1(*c*) shows a sawtooth waveform for $E_0 = 1.5$, with the period of the wave being $T_w = 1.53\tau_c$ (frequency $f_w = 0.66 f_c$). For $E_0 = 3.5$ (figure 1*d*), a spiky bipolar waveform is shown, where the period of the wave is $T_w = 2.62\tau_c$ (frequency $f_w = 0.38 f_c$). It is noted that the period of the spiky structure is about two and a half times the cyclotron period and is consistent with the associated acoustic mode.

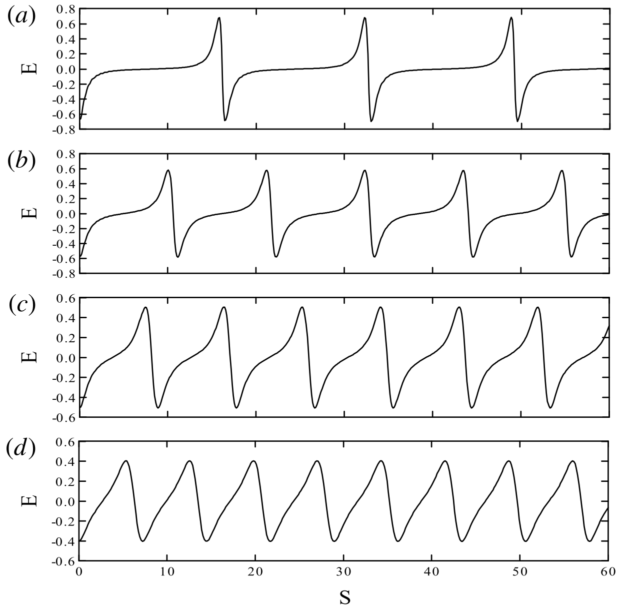

FIGURE 2. Numerical solution of the normalized electric field for the parameters $E_0 = 2.0$, $R = 10.0$, $\theta = 2^{\circ}$, $\delta_c = \delta_h = 0.0$, $n_{ec0}/n_0 = n_{pc0}/n_0 = 0.5$, $T_c/T_h = 0.0$, and $M =$ (*a*) 3.0, (*b*) 3.5, (*c*) 4.0 and (*d*) 5.0.

Figure 2(*a–d*) shows the effect of the Mach number on the electrostatic waves. Here M is varied from 3.0 to 5.0 with the fixed parameters, $E_0 = 2.0$, $R = 10.0$, $\theta = 2^{\circ}$, $\delta_c = \delta_h = 0.0$, $n_{ec0}/n_0 = n_{pc0}/n_0 = 0.5$ and $T_c/T_h = 0.0$. As the Mach number increases, the wave structure changes from a sharp spiky form to a more sawtooth-like form. This indicates that the level of nonlinearity decreases with increasing M given the sequence observed when E_0 is increased in figure 1(*a–d*). A similar behaviour of the structures going from spiky to becoming sinusoidal with increasing Mach number is also found by Lu *et al.* (2010) for e–p plasma (see figures 2 and 3 of their paper). Hence for larger values of M, a stronger E_0 is required to generate the spiky structures. Also noted is that the period of the wave decreases with an increase in the Mach number. For $M = 3.0$, which is the minimum value for which a periodic nonlinear waveform exists for the above fixed parameters, the wave has a period of $T_w = 2.62\tau_c$ (frequency $f_w = 0.38 f_c$), implying an associated driven acoustic mode. As the Mach number increases to 5.0, the period of the wave decreases to $1.15\tau_c$ (frequency $f_w = 0.87 f_c$), exhibiting a sawtooth type structure.

The effect of the drift velocities for the hot electron and positron components are shown in figure 3(*a–e*). The fixed parameters are $E_0 = 3.5$, $M = 3.5$, $R = 10.0$, $\theta = 2^{\circ}$, $\delta_c = 0.0$, $n_{ec0}/n_0 = n_{pc0}/n_0 = 0.5$ and $T_c/T_h = 0.0$. The period of the spiky structures decreases from $3.83\tau_c$ for $\delta_c = -0.3$ to $3.06\tau_c$ for $\delta_c = +0.3$. Here the hot electron and positron flow anti-parallel (parallel) to $\boldsymbol{B}_0$ increases (decreases) the period of the spiky structure. Previous studies on electron–ion plasmas showed a similar behaviour for the hot electron drift velocities (Reddy *et al.* 2002; Moolla *et al.* 2003). For the ESWs observed in the Earth's magnetosphere, it was found that the period of the ESWs changed rapidly (Kojima *et al.* 1994). Given the above found dependence of the periodicity on the hot electron drift speed, it has been suggested that the observed

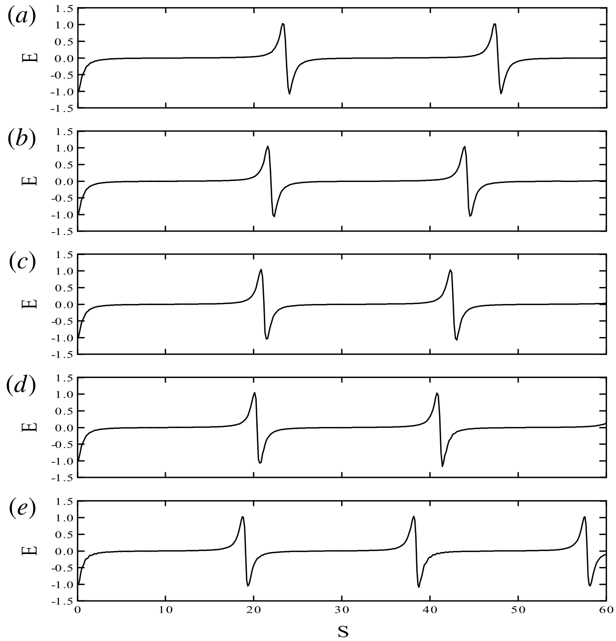

FIGURE 3. Numerical solution of the normalized electric field for the parameters $M = 3.5$, $E_0 = 3.5$, $R = 10.0$, $\theta = 2^\circ$, $n_{ec0}/n_0 = n_{pc0}/n_0 = 0.5$, $T_c/T_h = 0.0$, $\delta_c = 0$ and $\delta_h =$ (*a*) -0.3, (*b*) -0.1, (*c*) 0.0, (*d*) 0.1 and (*e*) 0.3.

rapid changes in the period of the ESWs could be due to electrons being accelerated in bursts (Moolla *et al.* 2003). Our results show that a similar phenomenon could occur in an e–p plasma where, due to the symmetry of the system, both species (electrons and positrons) are drifting.

Figure 4(*a–e*) show the variation of the drift velocities for the cool electron and positron components. The fixed parameters are $E_0 = 3.5$, $M = 3.5$, $R = 10.0$, $\theta = 2^\circ$, $\delta_h = 0.0$, $n_{ec0}/n_0 = n_{pc0}/n_0 = 0.5$ and $T_c/T_h = 0.0$. Here we observe that the period of the spiky structures increases from $2.89\tau_c$ for $\delta_c = -0.3$, to $4.17\tau_c$ for $\delta_c = +0.3$, i.e. as the cool beam flow becomes more parallel to the ambient magnetic field. Therefore, for anti-parallel flow to $\boldsymbol{B}_0$, the period of the spiky structure for the cool electrons and positrons decrease and for parallel flow it increases. It is noted that the effect of the cool electron and positron drift velocity on the ESWs is opposite to that compared to the hot electron and positron drift velocity on the waves, indicating that the period of the ESWs depends only on the relative velocity between the cool and hot species.

Figure 5(*a–d*) show the effect of the electron and positron densities on the normalized electric field. The fixed parameters are, $E_0 = 1.5$, $M = 3.5$, $R = 10.0$, $\theta = 2^\circ$, $\delta_c = \delta_h = 0.0$ and $T_c/T_h = 0.0$. As the densities n_{eco} and n_{pco} increase, the oscillations becomes more nonlinear, with increasing periodicity. With $n_{eco} = n_{pco} = 0.1$, a linear waveform of period $1.01\tau_c$ (frequency $f_w = 0.99f_c$) is observed. As the densities are increased ($n_{eco} = n_{pco} = 0.4$), the waveform tends to a sawtooth structure of period $1.22\tau_c$ (frequency $f_w = 0.82f_c$). For even larger densities ($n_{eco} = n_{pco} = 0.7$), the electric field evolves into a spiky structure of period $2.66\tau_c$ (frequency $f_w = 0.38f_c$). It is noted that a smaller driving electric field is required to drive the nonlinearity of the wave for larger density values. Since the periods of the waves are greater than $1.0\tau_c$, these waves are associated with a driven acoustic mode.

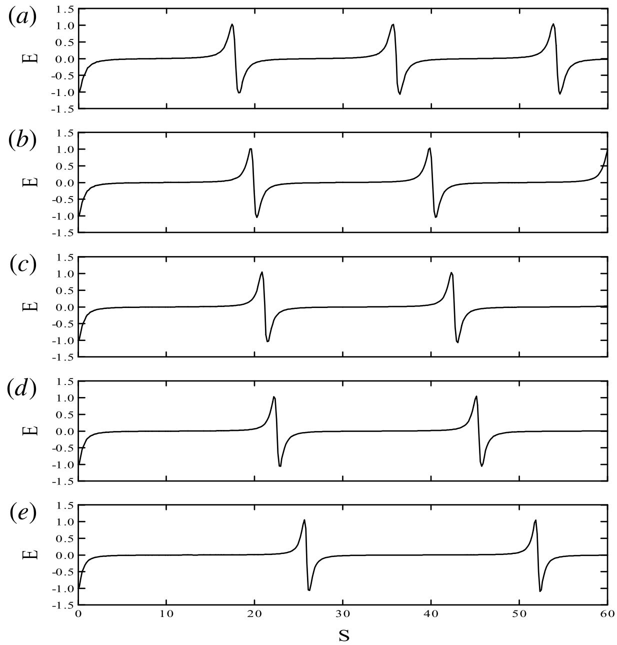

FIGURE 4. Numerical solution of the normalized electric field for the parameters $M = 3.5$, $E_0 = 3.5$, $R = 10.0$, $\theta = 2^\circ$, $n_{ec0}/n_0 = n_{pc0}/n_0 = 0.5$, $T_c/T_h = 0.0$, $\delta_h = 0$ and $\delta_c =$ (*a*) -0.3, (*b*) -0.1, (*c*) 0.0, (*d*) 0.1 and (*e*) 0.3.

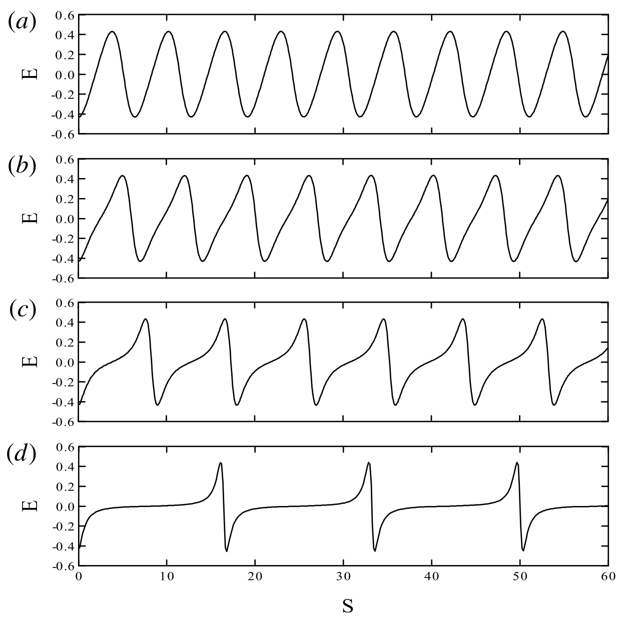

FIGURE 5. Numerical solution of the normalized electric field for the parameters $M = 3.5$, $E_0 = 1.5$, $R = 10.0$, $\theta = 2^\circ$, $\delta_c = \delta_h = 0.0$, $T_c/T_h = 0.0$, and $n_{ec0}/n_0 = n_{pc0}/n_0 =$ (*a*) 0.1, (*b*) 0.3, (*c*) 0.5 and (*d*) 0.7.

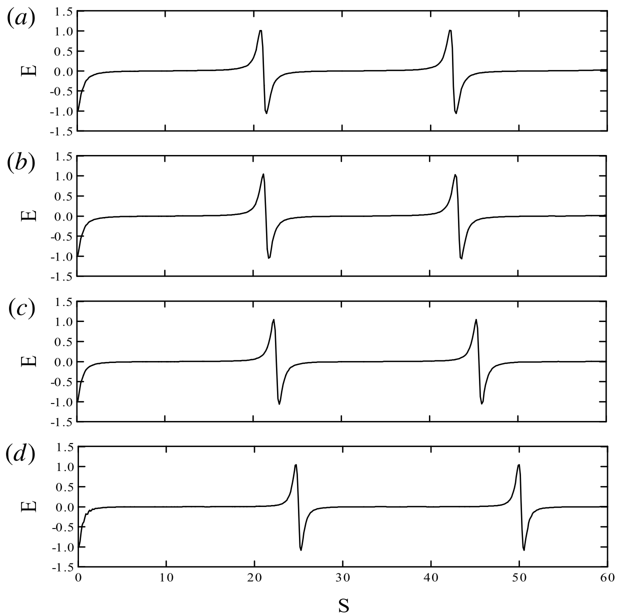

FIGURE 6. Numerical solution of the normalized electric field for the parameters with $M = 3.5$, $E_0 = 3.5$, $R = 10.0$, $\theta = 2^\circ$, $\delta_c = \delta_h = 0.0$, $n_{ec0}/n_0 = n_{pc0}/n_0 = 0.5$, and $T_c/T_h =$ (*a*) 0.0, (*b*) 0.25, (*c*) 0.5 and (*d*) 0.75.

In figure 6(*a–d*) we examine the effect of the cool-to-hot electron and positron temperature ratio on the waves. The fixed parameters are, $E_0 = 3.5$, $M = 3.5$, $R = 10.0$, $\theta = 2^\circ$, $\delta_c = \delta_h = 0.0$ and $n_{ec0}/n_0 = n_{pc0}/n_0 = 0.5$. Here the periodicity and nonlinearity of the wave increases with an increase in the cool-to-hot temperature ratio. The period of the wave increases from $3.42\tau_c$ (frequency $f_w = 0.29f_c$) for $T_c/T_h = 0.0$ to $4.02\tau_c$ (frequency $f_w = 0.25f_c$) for $T_c/T_h = 0.75$. This effect may be seen from the linear dispersion relation (2.11), where as the temperature increases, ω decreases and hence the period of the wave increases.

In figure 7(*a–d*), we have varied the propagation angle θ. The fixed parameters are $E_0 = 3.5$, $M = 3.5$, $R = 10.0$, $\delta_c = \delta_h = 0.0$, $n_{ec0}/n_0 = n_{pc0}/n_0 = 0.5$ and $T_c/T_h = 0.0$. The oscillations are of a spiky nature and the periodicity of the wave remains unchanged with a period of $2.75\tau_c$ (frequency $f_w = 0.36f_c$), representing an associated acoustic mode. As the propagation angle increases with respect to $\boldsymbol{B}_0$, the wave becomes increasingly more distorted with a double-humped feature. The maximum propagation angle that produced a reasonably periodic waveform of this type was found to be 35°.

An examination of the critical driving electric field amplitudes for the onset of spiky electrostatic waves as a function of the Mach number for various density ratio values was conducted for the fixed parameters $R = 10.0$, $\delta_c = \delta_h = 0.0$, $T_c/T_h = 0.0$ and $\theta = 2^\circ$. It is noted that as the Mach number increases, a larger driving electric field amplitude is required for the onset of the spiky electrostatic waves. The increase of E_0 with M is much sharper for lower values of n_{ec0} $(= n_{pc0})$. Also as the density ratio increases for a fixed Mach number, the critical driving electric field amplitude for the onset of spiky ESWs decreases. Further, with an increase in the density ratio, the minimum value required for the wave speed decreases for the onset of spiky ESWs.

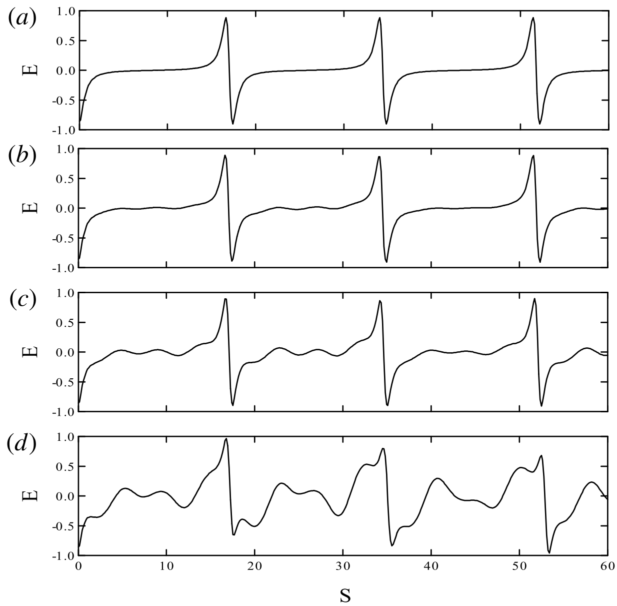

FIGURE 7. Numerical solution of the normalized electric field for the parameters $M = 3.5$, $E_0 = 3.5$, $R = 10.0$, $n_{ec0}/n_0 = n_{pc0}/n_0 = 0.5$, $\delta_c = \delta_h = 0.0$, $T_c/T_h = 0.0$, and $\theta =$ (*a*) 2°, (*b*) 10°, (*c*) 20°, (*d*) 35°.

An examination of the period and pulse width of the electrostatic wave as a function of the drift velocities for the cold electron and positron components (δ_c) was also conducted for the fixed parameters $M = 3.5$, $E_0 = 3.5$, $R = 10.0$, $n_{ec0}/n_0 = n_{pc0}/n_0 = 0.5$, $\delta_h = 0.0$, $T_c/T_h = 0.0$ and $\theta = 2°$. It is noted that as the drift velocities for the cold electron and positron component goes from anti-parallel to parallel flow, the period and pulse width of the ESWs increases. This effect is opposite for the drift velocities of the hot electron and positron components, i.e. as you go from anti-parallel to parallel for the hot drift velocities δ_h, the period and pulse width decrease. Similar behaviour from satellite observations was reported, i.e. the period and pulse width decreased (Kojima *et al.* 1994). In their measurements, they found that the ratio w/T was a constant for the ESWs, with $w/T = 0.3$, where w is the pulse width and T is the period of the wave. In our studies, we found that the ratio w/T was also a constant, with $w/T \approx 0.96$.

4. Discussion

In this paper, we have investigated the evolution of nonlinear electrostatic solitary waves in a two-temperature magnetized e–p plasma. In the model considered, spatial variation is restricted to the x-direction, while the external magnetic field is in the (x, z) plane. In the nonlinear analysis, the associated cyclotron wave and acoustic wave are coupled through the convective derivative terms $v_{jx}(\partial v_{jy}/\partial x)$ and $v_{jx}(\partial v_{jz}/\partial x)$ in the momentum equations. These two modes are decoupled in the linear analysis. A transition from linear sinusoidal to sawtooth to spiky waveforms is observed as the amplitude of the driving electric field increases. The results found here for an e–p plasma are very similar to those found by other researchers for electron–ion plasmas. On the other hand, as the Mach number is increased (figure 2*a*–*d*) the nonlinearity is suppressed to the point where the bipolar ESWs are no longer excited. For the onset of spiky ESWs, it is noted that as the wave speed increases, a larger driving electric field is required. The periods of the waves are found to be affected by the relative drift between the hot and cold electrons and positrons. Also, the onset of nonlinear structures is affected by the density ratio of the cool-to-hot particle species. As the density ratio increases, the critical value for the driving electric field amplitude for the onset of spiky ESWs decreases and the minimum value required for the wave speed for the onset of spiky ESWs also decreases. The ESWs are therefore more easily excited where the cool species dominate. The results further show that ESWs exists for almost parallel propagation, but as the propagation angle increases with respect to the ambient magnetic field $\boldsymbol{B}_0$, the signature waveform becomes more distorted, with a double-humped feature. The ratio of the pulse widths and periods (w/T) of the electrostatic waves was found to be a constant, which is consistent with experimental observations (Kojima *et al.* 1994) and as found for a plasma consisting of cold and hot electrons and ions (Moolla *et al.* 2007). When finite temperature effects are included, an increase in the temperature ratio of the cool-to-hot electrons and positrons causes the broadening out of the waveforms, which variation is associated with an increase in the wave frequency with T_c. The nonlinear electrostatic spiky structures studied here may have important implications for pulsars radiation and their microstructure. Firstly, these ESW can modulate the pulsar electromagnetic radiation with a periodicity of T_w (varying from 1 to 5 times the cyclotron period) leading to some microstructures via modulational instabilities (Hasegawa 1975; Luo 1998). These fine structures could have a constant $w/T = 0.96$. Secondly, the ESWs can couple with the electromagnetic waves and produce a new source of pulsar radiation as discussed by Stark *et al.* (2007).

Here, we have not included the electromagnetic and relativistic effects in this paper. However, in the non-relativistic plasma case discussed here, these effects are not expected to be important as both the cyclotron and acoustic modes are electrostatic. The general case of the coupling between electrostatic and electromagnetic modes is quite complex and beyond the scope of this paper.

Acknowledgements

G.S.L. thanks the National Academy of Sciences, India for the support under the NASI-Senior Scientist Platinum Jubilee Fellowship.

REFERENCES

ASSEO, E. & RIAZUELO, A. 2000 Relativistic anisotropic pair plasmas. *Mon. Not. R. Astron. Soc.* **318**, 983–1004.

BHARUTHRAM, R. 1992 Arbitrary amplitude double layers in a multi-species electron–positron plasma. *Astrophys. Space Sci.* **189**, 213–222.

BHATTACHARYYA, R., JANAKI, M. S. & DASGUPTA, B. 2003 Relaxation in electron–positron plasma: a possibility. *Phys. Lett.* A **315**, 120–125(6).

ERGUN, R. E., CARLSON, C. W., MCFADDEN, J. P., MOZER, F. S., DELROY, G. T., PERIA, W., CHASTON, C. C., TEMERIN, M., ELPHIC, R., STRANGEWAY, R. *et al.* 1998 FAST satellite observations of large-amplitude solitary wave structures. *Geophys. Res. Lett.* **25**, 2041–2044.

ESFANDYARI-KALEJAHI, A., KOURAKIS, Y. & SHUKLA, P. K. 2006 Oblique modulation of electrostatic modes and envelope excitations in pair-ion and electron–positron plasmas. *Phys. Plasmas* **13**, 122310–122318.

FRANZ, J. R., KINTNER, P. M. & PICKETT, J. S. 1998 POLAR observations of coherent electric field structures. *Geophys. Res. Lett.* **25**, 1277–1280.

GOLDREICH, P. & JULIAN, W. H. 1969 Pulsar electrodynamics. *Astrophys. J.* **157**, 869–880.

GREAVES, R. G. & SURKO, C. M. 1995 An electron–positron beam-plasma experiment. *Phys. Rev. Lett.* **75**, 3846–3849.

HASEGAWA, A. 1975 *Plasma Instabilities and Nonlinear Effects*, p. 194. Springer.

IWAMOTO, N. 1993 Collective modes in nonrelativistic electron–positron plasmas. *Phys. Rev.* E **47**, 604–611.

KASHIYAMA, K., IOKA, K. & KAWANAKA, N. 2011 White dwarf pulsars as possible cosmic ray electron–positron factories. *Phys. Rev.* D **83**, 023002–023022.

KOJIMA, H., MATSUMOTO, H., MIYATAKE, T., NAGANO, I., FUJITA, A., FRANK, L. A., MUKAI, T., PATERSON, W. R., SAITO, Y., MACHIDA, S. *et al.* 1994 Relation between electrostatic solitary waves and hot plasma flow in the plasma sheet boundary layer: GEOTAIL observations. *Geophys. Res. Lett.* **21**, 2919–2922.

KOJIMA, H., OHTSUKA, K., MATSUMOTO, H., OMURA, Y., ANDERSON, R. R., SAITO, Y., MUKAI, T., KOKUBUN, S. & YAMAMOTO, T. 1999 Plasma waves in slow-mode shocks observed by GEOTAIL spacescraft. *Adv. Space Res.* **24**, 51–54.

LAZARUS, I. J., BHARUTHRAM, R. & HELLBERG, M. A. 2008 Modified Korteweg–de Vries–Zakharov–Kuznetsov solitons in symmetric two-temperature electron–positron plasmas. *J. Plasma Phys.* **74**, 519–529.

LAZARUS, I. J., BHARUTHRAM, R., SINGH, S. V., PILLAY, S. R. & LAKHINA, G. S. 2012 Linear electrostatic waves in two temperature electron–positron plasmas. *J. Plasma Phys.* **78**, 621–628.

LIU, Y. & LIU, S. Q. 2011 Nonlinear behavior of electromagnetic waves in ultra-relativistic electron–positron plasmas. *Contrib. Plasma Phys.* **51**, 698–706.

LU, G., LIU, Y., WANG, Y., STENFLO, L., POPEL, S. I. & YU, M. Y. 2010 Fully nonlinear electrostatic waves in electron–positron plasmas. *J. Plasma Phys.* **76**, 267–275.

LUO, Q. 1998 Plasma processes in pulsar magnetospheres and eclipsing binary pulsar systems. *Braz. J. Phys.* **28**, 191–202.

MATSUMOTO, H., KOJIMA, H., KASABA, Y., MIYAKE, T., ANDERSON, R. R. & MUKAI, T. 1997 Plasma waves in the upstream and bow shock regions observed by GEOTAIL. *Adv. Space Res.* **20**, 683–693.

MATSUMOTO, H., KOJIMA, H., MIYATAKE, T., OMURA, Y., OKADA, M., NAGANO, I. & TSUTSUI, M. 1994 Electrostatic solitary waves (ESW) in the magnetotail: BEN wave forms observed by GEOTAIL. *Geophys. Res. Lett.* **21**, 2915–2918.

MICHEL, F. C. 1982 Theory of pulsar magnetospheres. *Rev. Mod. Phys.* **54**, 1–66.

MILLER, H. R. & WITTA, P. J. 1987 *Active Galactic Nuclei*, p. 202. Springer.

MOFIZ, U. A. & AMIN, M. R. 2013 Langmuir dark solitons in dense ultrarelativistic electron–positron gravito-plasma in pulsar magnetosphere. *Astrophys. Space Sci.* **345**, 119–124.

MOFIZ, U. A. & MAMUN, A. A. 1992 Spiky Langmuir solitons in a dense ultrarelativistic electron–positron plasma. *Phys. Fluids* B **4**, 3806–3807.

MOOLLA, S., BHARUTHRAM, R., SINGH, S. V. & LAKHINA, G. S. 2003 Non-linear high-frequency waves in the magnetosphere. *Pramana J. Phys.* **61**, 1209–1214.

MOOLLA, S., BHARUTHRAM, R., SINGH, S. V., LAKHINA, G. S. & REDDY, R. V. 2007 An explanation for high-frequency broadband electrostatic noise in the Earth's magnetosphere. *J. Geophys. Res.* **112**, A07214p1-23.

OMURA, Y., KOJIMA, H. & MATSUMOTO, H. 1994 Computer simulation of electrostatic solitary waves: a nonlinear model of broadband electrostatic noise. *Geophys. Res. Lett.* **21**, 2923–2926.

PIRAN, T. 2005 The physics of gamma-ray bursts. *Rev. Mod. Phys.* **76**, 1143–1210.

PRESS, W. H., TEUKOLSKY, S. A., VETTERLING, W. T. & FLANNERY, B. P. 1996 *Numerical Receipes in Fortran 90 – 'The Art of Parallel Scientific Computing'*, vol. 2, pp. 702–704, 731, 740, 1297, 1308. Cambridge University Press.

REDDY, R. V., LAKHINA, G. S., SINGH, N. & BHARUTHRAM, R. 2002 Spiky parallel electrostatic ion cyclotron and ion acoustic waves. *Nonlinear Process. Geophys.* **9**, 25–29.

STARK, C. R., DIVER, D. A., DA COSTA, A. A. & LAING, E. W. 2007 Nonlinear mode coupling in pair plasmas. *Astron. Astrophys.* **476**, 17–30.

STURROCK, P. A. 1971 A model of pulsars. *Astrophys. J.* **164**, 529–556.

TEMERIN, M. A., CERNY, K., LOTKO, W. & MOZER, F. S. 1982 Observations of double layers and solitary waves in the auroral plasma. *Phys. Rev. Lett.* **48**, 1175–1179.

VERHEEST, F., HELLBERG, M. A., GRAY, G. J. & MACE, R. L. 1996 Electrostatic solitons in multispecies electron–positron plasmas. *Astrophys. Space Sci.* **239**, 125–139.

WEISE, J. & MELROSE, D. B. 2002 One-photon pair production in pulsars: non-relativistic and relatrivistic regimes. *Mon. Not. R. Astron. Soc.* **329**, 115–125.

ZANK, G. P. & GREAVES, R. G. 1995 Linear and nonlinear modes in nonrelativistic electron–positron plasmas. *Phys. Rev.* E **51**, 6079–6090.